Hmgb3 regulates the balance between hematopoietic stem cell self-renewal and differentiation

Michael J. Nemeth, Martha R. Kirby, and David M. Bodine

PNAS 2006;103;13783-13788; originally published online Aug 31, 2006;
doi:10.1073/pnas.0604006103

Hmgb3 regulates the balance between hematopoietic stem cell self-renewal and differentiation

Michael J. Nemeth, Martha R. Kirby, and David M. Bodine*

Hematopoiesis Section, Genetics and Molecular Biology Branch, National Human Genome Research Institute, Bethesda, MD 20892-4442

Edited by Ernest Beutler, The Scripps Research Institute, La Jolla, CA, and approved July 25, 2006 (received for review May 15, 2006)

Hmgb3 is an X-linked member of a family of sequence-independent chromatin-binding proteins that is preferentially expressed in hematopoietic stem cells (HSC). *Hmgb3*-deficient mice (*Hmgb3*$^{-/Y}$) contain normal numbers of HSCs, capable of self-renewal and hematopoietic repopulation, but fewer common lymphoid (CLP) and common myeloid progenitors (CMP). In this study, we tested the hypothesis that *Hmgb3*$^{-/Y}$ HSCs are biased toward self-renewal at the expense of progenitor production. Wild-type and *Hmgb3*$^{-/Y}$ CLPs and CMPs proliferate and differentiate equally *in vitro*, indicating that CLP and CMP function normally in *Hmgb3*$^{-/Y}$ mice. *Hmgb3*$^{-/Y}$ HSCs exhibit constitutive activation of the canonical Wnt signaling pathway, which regulates stem cell self-renewal. Increased Wnt signaling in *Hmgb3*$^{-/Y}$ HSCs corresponds to increased expression of *Dvl1*, a positive regulator of the canonical Wnt pathway. To induce hematopoietic stress and a subsequent response from HSCs, we treated *Hmgb3*$^{-/Y}$ mice with 5-fluorouracil. *Hmgb3*$^{-/Y}$ mice exhibit a faster recovery of functional HSCs after administration of 5-fluorouracil compared with wild-type mice, which may be due to the increased Wnt signaling. Furthermore, the recovery of HSC number in *Hmgb3*$^{-/Y}$ mice occurs more rapidly than CLP and CMP recovery. From these data, we propose a model in which *Hmgb3* is required for the proper balance between HSC self-renewal and differentiation.

hematopoiesis | Wnt

Hematopoietic stem cells (HSC) are a rare population of cells that predominantly reside within adult bone marrow and are responsible for life-long replenishment of all blood cell types (1). HSCs differentiate into common lymphoid (CLP) and common myeloid progenitors (CMP) that are capable of exponential proliferation and differentiation. To maintain their numbers, HSCs undergo self-renewal, which generates progeny that retain the ability for multilineage differentiation. The mechanisms by which the fate of HSCs, either self-renewal or differentiation, is determined are still unclear.

The proteins that comprise the high-mobility group (HMG) superfamily are among the most abundant nonhistone proteins in the eukaryotic nucleus (2). Hmgb3 is an X-linked member of this superfamily and is classified with Hmgb1 and -2 into the Hmg-box subfamily, defined by the presence of DNA-binding Hmg-box domains (3). The 80% identity between Hmg-box proteins (4), suggests similar functions at the molecular level. Hmgb1 and -2 have been shown to bind DNA without sequence specificity and can bend linear DNA (5, 6). They also interact directly with Hox and Oct family transcription factors, which have been reported to be important regulators of stem cell differentiation (7–10).

Hmgb1, *-2*, and *-3* exhibit different patterns of gene expression in the adult mouse. *Hmgb1* expression is ubiquitous, *Hmgb2* is primarily expressed in the thymus and testes, and *Hmbg3* expression is localized to the bone marrow (4, 11, 12). The tissue-specific expression patterns may be responsible for the phenotypes observed in mouse knockout models. *Hmgb1* deficiency results in lethal hypoglycemia in newborn mice and, whereas *Hmgb2*$^{-/-}$ mice are viable, homozygous males exhibit decreased fertility because of defective spermatogenesis (4, 11).

In adult bone marrow, *Hmgb3* is found in maturing Ter119^{+} erythroid cells and in populations enriched for HSCs, CLPs, and CMPs (12). *Hmgb3* is a marker for HSCs, whereas lin^{-}, c-kit^{HI}, and *Hmgb3*^{NEG} cells were incapable of long-term bone marrow repopulation. *Hmgb3*-deficient mice (*Hmgb3*$^{-/Y}$) are viable and hematologically normal except for a mild erythrocythemia (13). *Hmgb3*$^{-/Y}$ mice contain normal numbers of HSCs, which are capable of self-renewal and long-term repopulation. However, there are reduced numbers of CLPs and CMPs in *Hmgb3*$^{-/Y}$ mice, which is compensated by increased proliferation of more mature progenitors, resulting in normal numbers of hematopoietic cells.

The canonical Wnt signaling pathway regulates proliferation and differentiation of several cellular systems, including multiple types of stem cells (reviewed in Logan and Nusse, ref. 14). In this pathway, binding of Wnt ligand to its cognate receptor leads to activation of the Dishevelled (Dvl1) protein, which ultimately causes stabilization and nuclear translocation of β-catenin and the subsequent induction of target gene expression. Activation of this pathway has been shown to increase HSC and leukemia stem cell self-renewal (15, 16).

In this study, we have focused on the role of *Hmgb3* in regulating cell-fate decisions of HSCs. We hypothesized that the reduction in CLP and CMP numbers in *Hmgb3*$^{-/Y}$ mice may be because of either more rapid differentiation of CLPs and CMPs or decreased production of CLPs and CMPs. We observed that CLPs and CMPs from wild-type and *Hmgb3*$^{-/Y}$ mice proliferate and differentiate at similar rates, leading us to hypothesize that the decreased numbers of CLPs and CMPs were because of their impaired production by the HSC. We observed enhanced activation of the canonical Wnt signaling pathway in *Hmgb3*-deficient HSCs. Consistent with this observation, *Hmgb3*-deficient HSCs contain increased levels of *Dvl1* mRNA. We compared the effects of 5-fluorouracil (5-FU), which transiently eliminates c-kit^{HI} cells, on HSC, CLP, and CMP populations in wild-type and *Hmgb3*$^{-/Y}$ mice (17). After 5-FU treatment, c-kit^{HI} HSCs in *Hmgb3*$^{-/Y}$ mice recovered more rapidly than in wild-type mice. Furthermore, recovery of c-kit^{HI} hematopoietic progenitors in *Hmgb3*$^{-/Y}$ mice was biased in favor of HSCs over CLPs and CMPs. Together, our data suggest that *Hmgb3* deficiency biases HSCs toward self-renewal at the expense of differentiation, and that the normal function of *Hmgb3* is to regulate the balance between these cell-fate decisions.

Results

Analysis of CLP and CMP Function in *Hmgb3*-Deficient Mice. We hypothesized that the reduced number of phenotypic CLP and CMP in *Hmgb3*$^{-/Y}$ mice may be caused by rapid differentiation of *Hmgb3*$^{-/Y}$ CLP and CMP, resulting in fewer cells with the typical CLP or CMP phenotype. To test this hypothesis, we performed *in*

IMMUNOLOGY

Conflict of interest statement: No conflicts declared.

This paper was submitted directly (Track II) to the PNAS office.

Abbreviations: 5-FU, 5-fluorouracil; CFU-GM, CFU-granulocyte–macrophage; CLP, common lymphoid progenitor; CMP, common myeloid progenitor; HMG, high-mobility group; HSC, hematopoietic stem cell; SP, side population.

*To whom correspondence should be addressed. E-mail: tedyaz@nhgri.nih.gov.

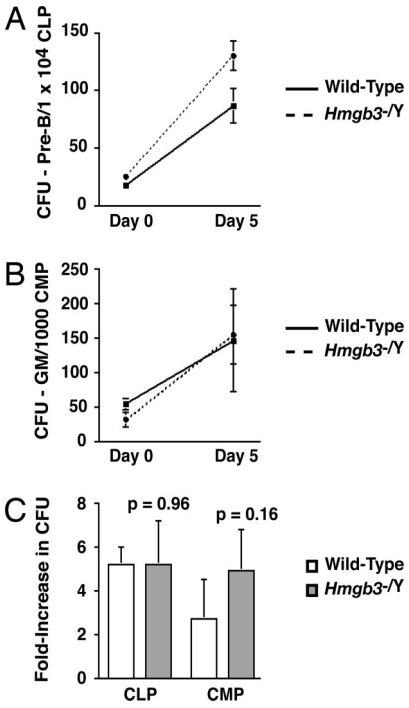

Fig. 1. Expansion of CLP and CMP *in vitro*. (*A*) Mean CFU-Pre-B frequency generated from CLPs (lin$^-$, c-kit^{LO}, Sca-1^{LO}, and IL-7Rα^+) before (day 0) and after 5 days in culture (day 5). CFU-Pre-B frequency was determined by scoring CFU-Pre-B per 1×10^4 CLP at day 0 and at day 5. Wild-type, $n = 12$, 212 colonies counted on day 0, 1,038 colonies counted on day 5; *Hmgb3*$^{-/Y}$, $n = 12$, 306 colonies counted on day 0, 1,563 colonies counted on day 5. The data represent the pooled results of three independent experiments. Error bars represent standard deviations. (*B*) Mean CFU-GM frequency generated from CMPs (lin$^-$, c-kit$^+$, Sca-1$^-$, and IL-7Rα^-) before (day 0) and after 5 days in culture (day 5). CFU-GM frequency was determined by scoring CFU-GM per 1,000 CMP at day 0 and at day 5. Wild-type, $n = 12$, 646 colonies counted on day 0, 1,755 colonies counted on day 5; *Hmgb3*$^{-/Y}$, $n = 12$, 377 colonies counted on day 0, 1,854 colonies counted on day 5. The data represent the pooled results of three independent experiments. Error bars represent standard deviations. (*C*) Average expansion in CFU generated by CLP and CMP before and after 5 days in culture ($n = 3$). The expansion in the number of CFU for each individual experiment was calculated by dividing the average CFU frequency at day 5 by the average CFU frequency at day 0. Error bars represent standard error of the mean. *P* values were generated by Student's *t* test.

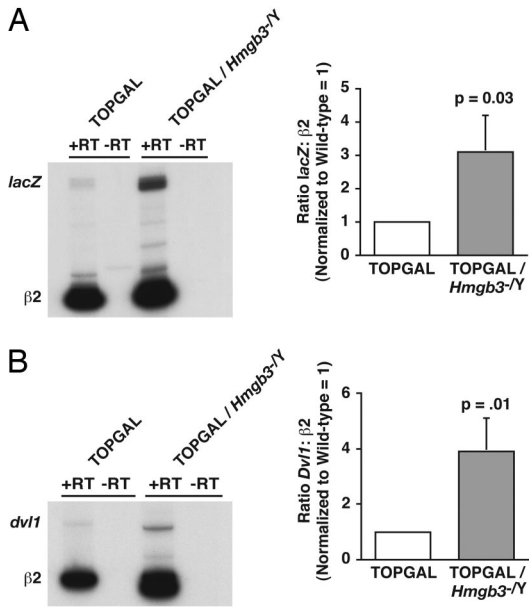

Fig. 2. Increased canonical Wnt signaling in *Hmgb3*$^{-/Y}$ HSCs after 5-FU treatment. (*A*) (*Left*) Semiquantitative duplex RT-PCR analysis of β-galactosidase mRNA in TOPGAL (wild-type) and TOPGAL $\times$ *Hmgb3*$^{-/Y}$ HSCs (lin$^-$, SP$^+$, c-kit^{HI}, Sca-1^{HI}, and IL-7Rα^-). Test gene mRNA levels were quantified within the linear range of amplification by densitometry and normalized to β2-microglobulin expression. (*Right*) β-Galactosidase mRNA levels relative to β2-microglobulin. The amount of β-galactosidase (lacZ) mRNA in TOPGAL ($n = 3$) and TOPGAL $\times$ *Hmgb3*$^{-/Y}$ ($n = 3$) HSCs was normalized to β2-microglobulin mRNA (β2) by the formula (densitometry value, test; densitometry value, β2-microglobulin). The normalized TOPGAL β-galactosidase mRNA level was then set to 1. The data represent the pooled results of three independent experiments by using mRNA isolated from sorted HSCs pooled from three mice. *P* values were determined by Student's *t* test. (*B*) (*Left*) Semiquantitative duplex RT-PCR analysis of *Dvl1* mRNA in wild-type TOPGAL and TOPGAL $\times$ *Hmgb3*$^{-/Y}$ HSCs (lin$^-$, SP$^+$, c-kit^{HI}, Sca-1^{HI}, and IL-7Rα^-). Test gene mRNA levels were quantified within the linear range of amplification by densitometry and normalized to β2-microglobulin expression. (*Right*) *Dvl1* mRNA levels relative to β2-microglobulin. The amount of *Dvl1* mRNA in TOPGAL ($n = 3$) and TOPGAL $\times$ *Hmgb3*$^{-/Y}$ ($n = 3$) HSCs was normalized to β2-microglobulin mRNA as described above.

vitro"delta" assays (18, 19), in which the formation of clonogenic colonies derived from CLPs (lin$^-$, c-kit$^+$, Sca-1$^+$, and IL-7Rα^+; ref. 20) and CMPs (lin$^-$, c-kit$^+$, Sca-1$^-$, IL-7Rα^-; ref. 21) isolated from *Hmgb3*$^{-/Y}$ and littermate control mice were compared before and after 5 days of expansion in serum-free culture.

Cultured *Hmgb3*$^{-/Y}$ and wild-type CLPs proliferated equivalently in culture (1.3 $\pm$ 0.2- and 1.4 $\pm$ 0.6-fold, respectively; $P = 0.7$). CFU-pre-B formation by wild-type and *Hmgb3*$^{-/Y}$ CLP also increased equivalently after 5 days in culture (5.2 $\pm$ 0.8- and 5.2 $\pm$ 2.0-fold, respectively; $P = 0.96$; Fig. 1 *A* and *C*). Wild-type and *Hmgb3*$^{-/Y}$ CMPs proliferated equivalently (6.5 $\pm$ 2.2- and 5.7 $\pm$ 1.5-fold, respectively; $P = 0.6$). There was no significant difference in CFU-granulocyte–macrophage (CFU-GM) formation after 5 days in culture by *Hmgb3*$^{-/Y}$ CMP compared with wild-type (4.9 $\pm$ 1.9- and 2.7 $\pm$ 1.8-fold, respectively; $P = 0.16$; Fig. 1 *B* and *C*). These data indicate that under identical *in vitro* conditions, wild-type and *Hmgb3*$^{-/Y}$ CLP and CMP are functionally similar in regard to proliferation and differentiation.

Activation of Wnt Signaling Through Overexpression of Dvl1 in *Hmgb3*-Deficient HSC. Based on these data, we hypothesized that *Hmgb3*-deficient HSCs are biased toward self-renewal, resulting in a deficiency in CLP and CMP. The canonical Wnt signaling pathway has been reported to activate self-renewal pathways in HSCs and leukemia stem cells (15, 16). To test our hypothesis, we examined the status of the canonical Wnt signaling pathway in wild-type and *Hmgb3*-deficient HSCs containing a *lacZ* reporter gene that is specifically expressed when the canonical Wnt pathway is activated (TOPGAL; ref. 22). Using RT-PCR, we observed a 3.1 $\pm$ 1.1-fold ($P = 0.03$) increase in the amount of lacZ mRNA in steady-state HSCs [lin$^-$, side population$^+$ (SP; ref. 23), Sca-1$^+$, c-kit$^+$, and IL-7Rα^-] isolated from TOPGAL $\times$ *Hmgb3*$^{-/Y}$ F_1 mice compared with TOPGAL controls (Fig. 2*A*), indicating a higher level of Wnt signaling in *Hmgb3*-deficient HSCs.

To determine the mechanism of increased Wnt signaling in *Hmgb3*-deficient HSCs, we analyzed the mRNA levels of several components of the canonical Wnt pathway. Using RT-PCR, we observed a 3.9 $\pm$ 1.2-fold increase in *Dvl1* mRNA levels in *Hmgb3*-deficient HSCs compared with wild-type (Fig. 2*B*). We were unable to detect any differences in the mRNA levels of *Axin*, *APC*, and *Btrc*, which are negative regulators of Wnt signaling (data not shown).

Hmgb3 Is Expressed Specifically in c-kit$^-$ Cells with Long-Term Repopulating Activity After 5-FU Treatment. Randall and Weissman (17) have shown that 5-FU transiently alters the HSC phenotype

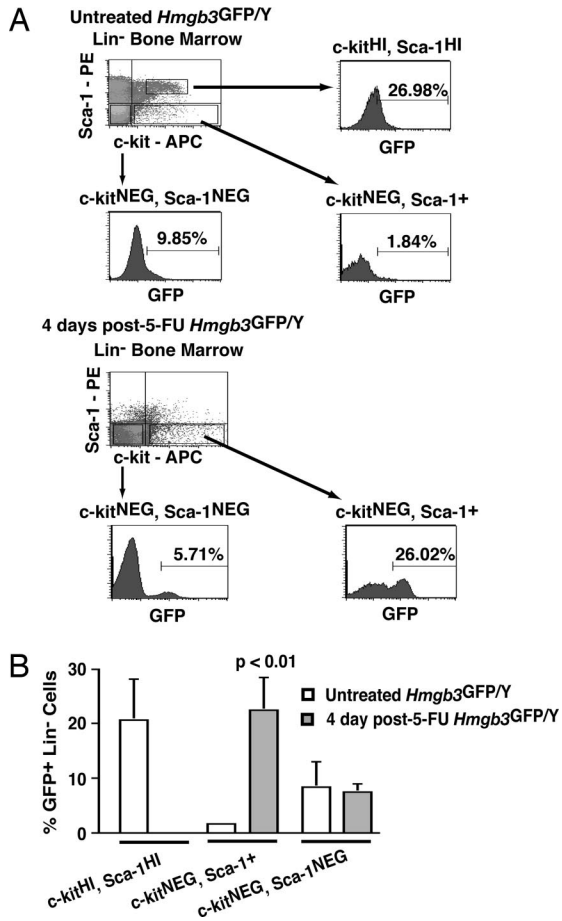

Fig. 3. Analysis of *Hmgb3* expression in primitive hematopoietic cells after 5-FU. (*A*) Representative FACS analysis of GFP$^+$ cells within various c-kit and Sca-1 populations in lin$^-$ bone marrow cells isolated from untreated *Hmgb3*$^{GFP/Y}$ mice and from *Hmgb3*$^{GFP/Y}$ mice 4 days after 5-FU administration. Regions were drawn based on isotype controls. (*B*) Average percentage of GFP$^+$ cells in lin$^-$ populations (c-kit^{HI}, Sca-1^{HI}; c-kit^{NEG}, Sca-1$^+$; c-kit^{NEG}, and Sca-1^{NEG}) from untreated *Hmgb3*$^{GFP/Y}$ mice and from *Hmgb3*$^{GFP/Y}$ mice 4 days after 5-FU administration. Bone marrow cells from three mice were pooled for each independent experiment; data represent the average of three experiments. Error bars represent standard deviation. *P* values were generated by Student's *t* test.

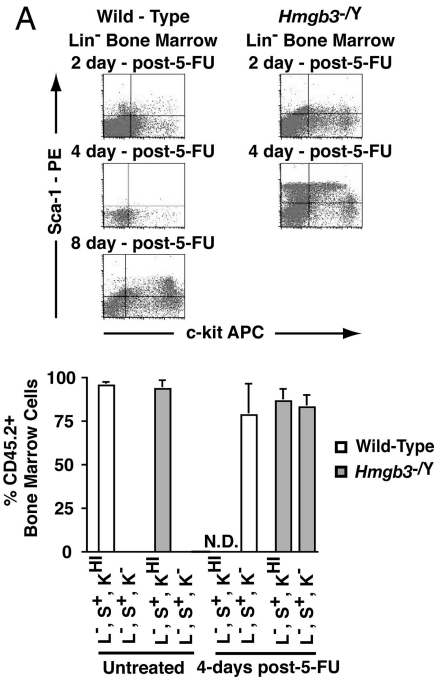

Fig. 4. Analysis of competitive repopulation assays. (*A*) Representative FACS profiles of c-kit$^+$ and Sca-1$^+$ populations within lin$^-$ bone marrow cells isolated from wild-type and *Hmgb3*$^{-/Y}$ mice 2, 4, and 8 days after treatment with 5-FU. Regions were drawn based on isotype controls. (*B*) FACS analysis was performed on bone marrow cells to determine the contribution to hematopoietic repopulation made by lin$^-$, Sca-1$^+$, c-kit^{HI}, or c-kit^{NEG} cells (CD45.2) isolated from untreated wild-type (c-kit^{HI}, $n = 3$; c-kit^{NEG}, $n = 3$) and *Hmgb3*$^{-/Y}$ (c-kit^{HI}, $n = 3$; c-kit^{NEG}, $n = 3$) mice and wild-type (c-kit^{NEG}, $n = 8$) and *Hmgb3*$^{-/Y}$ (c-kit^{HI}, $n = 8$; c-kit^{NEG}, $n = 8$) mice 4 days after 5-FU treatment. No experiment was performed by using c-kit^{HI} cells from wild-type mice 4 days after 5-FU treatment (ND) because of the lack of cells. Error bars represent standard deviation.

from c-kit^{HI} to c-kit$^{LO/NEG}$ followed by a reappearance of the c-kit^{HI} HSC after 8 days. According to our model, the HSCs in *Hmgb3*-deficient mice are actively engaging in self-renewal and should recover faster after 5-FU treatment than wild-type HSCs. We first established whether *Hmgb3* was expressed in c-kit^{NEG} HSCs after 5-FU treatment by monitoring *Hmgb3* expression in lin$^-$ cells isolated from phenotypically normal *Hmgb3*$^{GFP/Y}$ knockin mice before and after treatment with 5-FU. *Hmgb3*$^{GFP/Y}$ mice contain an internal ribosomal entry site-GFP cassette inserted into the 3′ UTR of *Hmgb3*, enabling the tracing of Hmgb3 expression through GFP (12).

Before 5-FU treatment, 20.6 ± 1.7% of lin-, c-kit^{HI}, and Sca-1^{HI} cells (HSCs) were GFP$^+$ as compared with 1.6 ± 0.4% of lin$^-$, c-kit$^-$, and Sca-1$^+$ cells and 8.3 ± 4.7% of lin$^-$, c-kit$^-$, and Sca-1$^-$ cells (Fig. 3 *A* and *B*). Four days after 5-FU treatment, lin$^-$, c-kit^{HI}, and Sca-1^{HI} cells were absent. There was a 14.5-fold increase in the number of lin$^-$, c-kit$^-$, and Sca-1$^+$ cells that were GFP$^+$ ($P < 0.01$). There was no change in the percentage of lin$^-$, c-kit$^-$, and Sca-1$^-$ cells that were GFP$^+$ (Fig. 3*B*). The increased proportion of GFP$^+$ lin$^-$, Sca-1$^+$, and c-kit$^-$ cells after 5-FU treatment is consistent with previous findings that repopulating activity resides within the c-kit$^{LO/NEG}$ population after 5-FU treatment, and that *Hmgb3* serves as a marker for long-term repopulating activity (12, 17). Furthermore, these results indicate that loss of *Hmgb3* has the potential to affect the c-kit^{NEG} population after 5-FU administration

We then compared the effects of 5-FU on *Hmgb3*-deficient and wild-type HSCs. As expected, 4 days after treatment of wild-type and *Hmgb3*$^{-/Y}$ mice with 5-FU, the c-kit^{HI} population was absent from wild-type lin$^-$ cells. However, numerous c-kit^{HI} and Sca-1$^+$ cells were present in *Hmgb3*$^{-/Y}$ lin$^-$ cells (Fig. 4*A*). To determine whether this effect was because of 5-FU resistance caused by higher levels of thymidylate synthase, we measured the levels of thymidylate synthase mRNA in wild-type and *Hmgb3*-deficient HSCs and found that the levels were identical (data not shown).

We analyzed repopulating activity of HSCs after 5-FU treatment isolated from untreated wild-type and *Hmgb3*$^{-/Y}$ mice and from wild-type and *Hmgb3*$^{-/Y}$ mice 4 days after 5-FU treatment. Lin$^-$, Sca-1$^+$, IL-7Rα^-, c-kit^{HI}, or c-kit^{NEG} candidate HSCs (CD45.2) were transplanted along with congenic bone marrow (CD45.1) cells into irradiated recipients. Twelve weeks after transplant, recipient bone marrow cells were analyzed by flow cytometry for contribution of donor (CD45.2) and competitor (CD45.1) HSCs to repopulation. Untreated wild-type and *Hmgb3*$^{-/Y}$ c-kit^{HI} cells repopulated recipients (95.1 ± 2.2% CD45.2$^+$ and 93.1 ± 5.0% CD45.2$^+$, respectively), but untreated c-kit^{NEG} cells did not (Fig. 4*B*). In agreement with previous results, 4 days after 5-FU treatment, lin$^-$, Sca-1$^+$, and c-kit^{NEG} cells isolated from wild-type mice provided all of the repopulating activity (78.4 ± 18.0% CD45.2$^+$; ref. 17). In contrast, 4

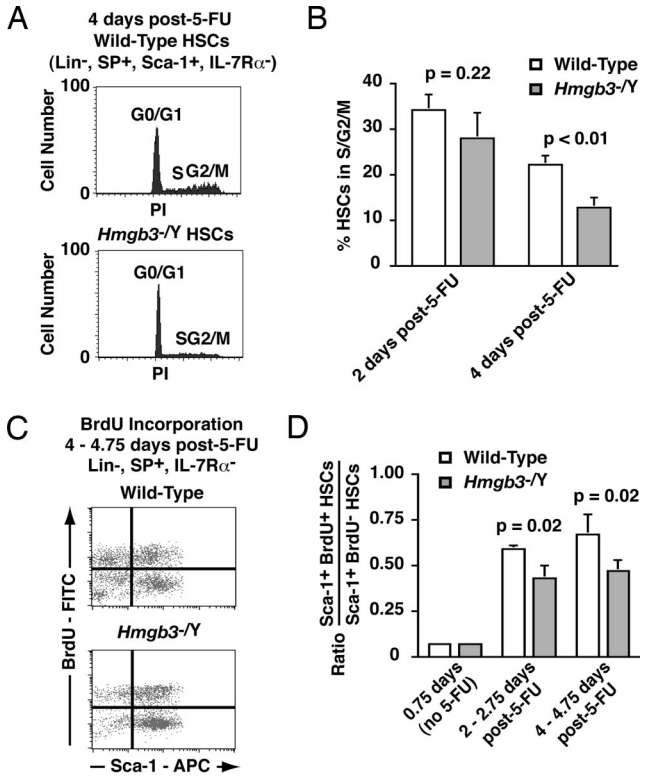

Fig. 5. Analysis of cell cycle status of *Hmgb3*$^{-/Y}$ HSCs after 5-FU. (*A*) Representative cell cycle histograms obtained through propidium iodide staining of HSCs (lin$^-$, SP$^+$, Sca-1$^+$, and IL-7Rα^-) isolated from wild-type and *Hmgb3*$^{-/Y}$ mice 4 days after 5-FU administration. Staining was performed on HSCs pooled from five mice for each group. Histograms were analyzed as described in *Materials and Methods*. (*B*) Average percentage of wild-type and *Hmgb3*$^{-/Y}$ HSCs in S/G_2/M phases of the cell cycle. HSCs were isolated from untreated wild-type and *Hmgb3*$^{-/Y}$ mice and from wild-type and *Hmgb3*$^{-/Y}$ mice 2 and 4 days after 5-FU administration. Data represent the average of three independent experiments for each group. Error bars represent standard deviation. *P* values were generated by Student's *t* test. (*C*) Representative FACS analysis of Sca-1$^+$ and BrdU$^+$ populations in lin$^-$, SP$^+$, and IL-7Rα^- cells isolated from wild-type and *Hmgb3*$^{-/Y}$ mice treated with 5-FU. Regions were drawn based on isotype controls. These analyses were performed on mice that were pulsed with a single dose of BrdU 4 days after treatment with 5-FU. Analyses were performed 18 h later, therefore Sca-1$^+$ and BrdU$^+$ cells represent HSCs that incorporated BrdU within the 18-h window. (*D*) Ratios of BrdU$^+$ to BrdU$^-$ HSCs (defined as lin$^-$, SP$^+$, and IL-7Rα^- that were also Sca-1$^+$) in untreated wild-type and *Hmgb3*$^{-/Y}$ mice (18-h window) and in wild-type and *Hmgb3*$^{-/Y}$ mice 2 days (BrdU pulse present for 2–2.75 days; $n = 3$) and 4 days (BrdU pulse present for 4–4.75 days; $n = 4$) after 5-FU treatment. Ratios were determined by the formula (no. BrdU$^+$ Sca-1$^+$ events/no. BrdU$^-$ Sca-1$^+$ events). Error bars represent standard deviations. *P* values were generated by Student's *t* test.

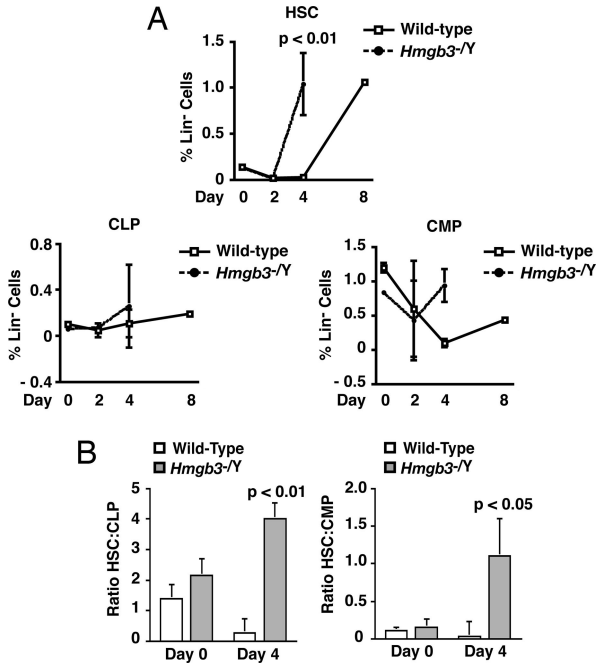

Fig. 6. Analysis of *Hmgb3*$^{-/Y}$ primitive hematopoietic cells after 5-FU treatment. (*A*) Average percentages of phenotypic primitive hematopoietic cells detected by FACS analysis in lin$^-$ cells isolated from untreated wild-type and *Hmgb3*$^{-/Y}$ mice and from wild-type and *Hmgb3*$^{-/Y}$ mice 2, 4, and 8 days after 5-FU treatment ($n = 4$ for all groups). (*Upper*) HSC (lin$^-$, c-kit^{HI}, Sca-1^{HI}, and IL-7Rα^-). (*Lower Left*) CLP (lin$^-$, c-kit^{LO}, Sca-1^{LO}, and IL-7Rα^+). (*Lower Right*) CMP (lin$^-$, c-kit$^+$, Sca-1$^-$, and IL-7Rα^-). Error bars represent standard deviations. *P* values were generated by Student's *t* test. (*B*) (*Left*) Ratio of HSCs to CLP in lin$^-$ cells from untreated wild-type and *Hmgb3*$^{-/Y}$ mice and from wild-type and *Hmgb3*$^{-/Y}$ mice 4 days after 5-FU treatment. (*Right*) Ratio of HSCs to CMP in lin$^-$ cells from untreated wild-type and *Hmgb3*$^{-/Y}$ mice and from wild-type and *Hmgb3*$^{-/Y}$ mice 4 days after 5-FU treatment. Ratios were determined by the formula (HSC [average % lin$^-$ cells)/CLP (or CMP) (average % lin$^-$ cells)]. Error bars represent standard deviations. *P* values were generated by Student's *t* test.

days after 5-FU treatment, both lin$^-$, Sca-1$^+$, and c-kit^{NEG} cells (86.3 ± 7.2% CD45.2$^+$) and lin-, Sca-1^{HI}, and ckit^{HI} cells (82.8 ± 6.9% CD45.2$^+$; $P = 0.60$, not significant) from *Hmgb3*$^{-/Y}$ mice demonstrated long-term repopulating ability. These results demonstrate a faster recovery of functional and phenotypic c-kit^{HI} HSCs in *Hmgb3*$^{-/Y}$ mice compared with wild-type.

Cell Cycle Status of *Hmgb3*-Deficient HSC After 5-FU Treatment. We hypothesized that after treatment with 5-FU, *Hmgb3*$^{-/Y}$ HSCs undergo self-renewal and return to a quiescent state sooner than wild-type HSCs. To test this, we performed cell cycle analyses on HSCs isolated from wild-type and *Hmgb3*$^{-/Y}$ mice 2 and 4 days after 5-FU treatment. Because c-kit cannot be used as an HSC marker in 5-FU-treated bone marrow, we used the side-population phenotype as an HSC marker instead, because this property is unaffected by 5-FU (24). Previously, we showed that 14.0% of untreated wild-type and 13.3% of *Hmgb3*$^{-/Y}$ HSCs are in the S/G_2/M phase (13). Two days after 5-FU treatment, there was no difference in the number of HSCs (lin$^-$, SP$^+$, Sca-1$^+$, and IL-7Rα^-) that were in the S/G_2/M phases of the cell cycle in wild-type mice (34.0 ± 3.4%) compared with *Hmgb3*$^{-/Y}$ mice (28.0 ± 5.6%; $P = 0.22$; Fig. 5 *A* and *B*). In contrast, 4 days after 5-FU treatment, there was a 50% decrease in the number of actively cycling HSCs in *Hmgb3*$^{-/Y}$ mice (12.6 ± 2.3%) compared with wild type (22.2 ± 1.9%; $P < 0.01$).

We also analyzed HSC proliferation by injecting *Hmgb3*$^{-/Y}$ and wild-type mice with BrdU at various time points after 5-FU administration (Fig. 5*C*). As we have shown previously, there was no difference in BrdU incorporation between steady-state wild-type and *Hmgb3*$^{-/Y}$ HSCs (ref. 13; Fig. 5*D*). The ratio of BrdU$^+$ to BrdU$^-$ HSCs was significantly increased in wild-type mice 18 h after a single pulse of BrdU was administered 2 days after 5-FU treatment compared with *Hmgb3*$^{-/Y}$ mice (0.60 ± 0.02 and 0.43 ± 0.07, respectively; $P = 0.02$). A similar increase was also observed 4 days after 5-FU treatment in wild-type mice (0.67 ± 0.11) compared with *Hmgb3*$^{-/Y}$ mice (0.48 ± 0.06; $P = 0.02$). Together, these data indicate decreased cell cycling and proliferation by *Hmgb3*$^{-/Y}$ HSCs 2–4 days after 5-FU administration and correlate with the percentage of HSCs in S/G_2/M.

Analysis of Effects of 5-FU on HSC and Primitive Progenitor Populations in *Hmgb3*-Deficient Mice. Because 5-FU depletes the bone marrow of cycling cells, which stimulates the HSC to begin pro-

duction of progenitors, we hypothesized that the reduction in CLP and CMP in *Hmgb3*$^{-/Y}$ mice was due to increased HSC generation at the expense of CLP and CMP. To test this, we used flow cytometry to compare the effects of 5-FU on the recovery of the HSC (lin$^-$, c-kit^{HI}, Sca-1^{HI}, and IL-7Rα^-), CLP (lin$^-$, c-kit^{LO}, Sca-1^{LO}, and IL-7Rα^+), and CMP (lin$^-$, c-kit$^+$, Sca-1$^-$, and IL-7Rα^-) populations in wild-type and *Hmgb3*$^{-/Y}$ mice. As shown in Fig. 4*A*, 4 days after 5-FU treatment, the number of phenotypic HSCs is increased in *Hmgb3*$^{-/Y}$ mice. We also observed a significant increase ($P < 0.01$) in the number of phenotypic CMPs in *Hmgb3*$^{-/Y}$ mice compared with wild-type (Fig. 6*A*). There was no difference in the number of phenotypic CLP.

To determine whether *Hmgb3*-deficient and wild-type HSCs favored self-renewal or production of progenitors upon activation, we measured the ratios of HSCs to CLPs and CMPs after 5-FU administration. An increase in the HSC to CLP and HSC to CMP ratios would lead us to conclude that self-renewal was favored over differentiation. In the steady state, the ratios of HSCs to CLPs in wild-type and *Hmgb3*$^{-/Y}$ mice were 1.41 ± 0.44 and 2.16 ± 0.53, respectively (Fig. 6*B*). Four days after 5-FU treatment, as expected, the HSC to CLP ratio in wild-type mice decreased to 0.27 ± 0.46, reflecting the relatively greater number of CLP. In contrast, in *Hmgb3*$^{-/Y}$ mice, this ratio increased to 4.0 ± 0.53 ($P < 0.01$) after 5-FU treatment. The ratios of HSC to CMP in wild-type and *Hmgb3*$^{-/Y}$ mice at steady state were 0.11 ± 0.05 and 0.15 ± 0.12, respectively (Fig. 6*B*). After 5-FU treatment, the wild-type HSC to CMP ratio decreased to 0.03 ± 0.02, whereas in *Hmgb3*$^{-/Y}$ mice, the HSC to CMP ratio increased to 1.1 ± 0.5 ($P < 0.05$).

Discussion

Previously, we demonstrated that *Hmgb3*-deficient mice have fewer CLPs and CMPs (13). It is possible that the decreased number of CLPs and CMPs in *Hmgb3*$^{-/Y}$ mice is due to increased apoptosis or rapid differentiation of CLPs and CMPs. However, the data generated by the "delta" assay do not support this conclusion. If the loss of *Hmgb3* enhanced CLP and CMP apoptosis, we expected to see decreased *in vitro* proliferation compared with wild-type progenitors. If *Hmgb3* deficiency caused a more rapid differentiation of CLP and CMP to a different phenotype or a stage with decreased ability to form clonogenic colonies, we expected to see a relative decrease in expansion of progenitor-derived CFU compared with wild-type. However, because we observed identical rates of CLP and CMP proliferation and expansion of CFU derived from *Hmgb3*$^{-/Y}$ and wild-type CLPs and CMPs, we concluded that *Hmgb3*$^{-/Y}$ and wild-type CLPs and CMPs are functionally identical.

Our hypothesis that *Hmgb3* deficiency biases HSCs toward self-renewal is supported by our observation that canonical Wnt signaling is increased in steady-state *Hmgb3*-deficient HSCs. Reya *et al.* (15) demonstrated that activation of the canonical Wnt pathway by recombinant Wnt ligand leads to HSC expansion. Similarly, overexpression of β-catenin increased self-renewal of leukemia stem cells isolated from chronic myelogenous leukemia patients (16). The increased activation of Wnt signaling may be because of the increased expression of *Dvl1* in *Hmgb3*-deficient HSCs, because overexpression of *dishevelled* has been shown to activate the Wnt pathway (25, 26). The increased level of Wnt signaling in steady-state *Hmgb3*-deficient HSCs may also contribute to the rapid expansion of ckit^{HI} and Sca-1^{HI} HSCs at the expense of progenitor production, as indicated by the increased ratios of HSCs to CLPs and CMPs in *Hmgb3*$^{-/Y}$ mice observed 4 days after 5-FU treatment.

Administration of 5-FU has been shown to affect HSC markers, such as the level of cell surface c-kit and rhodamine efflux (17, 24). The ability of *Hmgb3* to function as a stem cell marker is unaffected by treatment with 5-FU, because *Hmgb3* is expressed in the post-5-FU lin$^-$, c-kit^{NEG}, and Sca-1$^+$ population that contains the repopulating HSCs. Randall and Weissman (17) observed that, after treatment with 5-FU, the number of HSC is inversely correlated with the percentage of actively cycling HSCs. The rapid expansion of the c-kit^{HI} HSC population in *Hmgb3*$^{-/Y}$ mice is consistent with the decreased number of *Hmgb3*-deficient HSCs that are actively cycling and proliferating compared with wild type 4 days after 5-FU administration. From these data, we propose that during the first 48 h after 5-FU administration, wild-type and *Hmgb3*$^{-/Y}$ HSCs are actively dividing, but beyond 48 h, the increased numbers of Hmgb3-/Y HSCs begin to regain quiescence before the smaller number of wild-type HSCs.

Hmgb3 deficiency is correlated with increased *Dvl1* expression and activation of the canonical Wnt signaling pathway. Hmgb family members regulate chromatin structure and recruit proteins to DNA. We speculate that the observed increase in *Dvl1* expression is because of alterations in the normal chromatin architecture at the *Dvl1* locus, which subsequently activates Wnt signaling, allowing for increased HSC self-renewal and the generation of fewer CLP and CMP.

Materials and Methods

Mouse Strain Information. *Hmgb3*$^{GFP/Y}$ and *Hmgb3*$^{-/Y}$ mice (129/Sv strain) were generated as described (12, 13). TOPGAL mice (22) were kindly provided by Yingzi Yang (National Human Genome Research Institute, Bethesda, MD). 129SvEvTac and B6.SJL-*Ptprc*^{a}/BoAiTac mice were obtained from Taconic Farms (Germantown, NY).

Analysis of CLP and CMP Differentiation. CLPs (lin$^-$, c-kit^{LO}, Sca-1^{LO}, and IL-7Rα^+; ref. 20) were isolated from 8- to 10-week-old *Hmgb3*$^{-/Y}$ and littermate control mice, as described (12). Cells were sorted by using a FACSAria (Becton Dickinson, San Jose, CA) with 488-nm argon and 633-nm helium-neon lasers. Portions of sorted CLPs were cultured in Methocult M3630 methylcellulose, supplemented with 100 ng/ml stem cell factor (SCF) and 20 ng/ml human Flt3 ligand (Flt3L). The remainder was cultured in StemSpan media (StemCell Technologies, Vancouver, BC, Canada), supplemented with 100 ng/ml SCF/20 ng/ml Flt3L/20 ng/ml IL-7 (Peprotech, Rocky Hill, NJ) for 5 days before culturing in supplemented M3630 methylcellulose (StemCell Technologies). Methylcellulose cultures received equal numbers of input CLP before and after expansion. CFU-Pre-B assays were scored after 7 days. The expansion in the number of CLP-derived CFU-Pre-B after 5 days in culture was calculated by dividing the average number of CFU-Pre-B/1 × 10^4 CLP at day 5 by the average number of CFU-Pre-B/1 × 10^4 CLP at day 0. *P* values were generated by Student's *t* test.

CMPs (lin$^-$, c-kit$^+$, Sca-1$^-$, and IL-7Rα^-; ref. 21) were isolated from 8- to 10-week-old *Hmgb3*$^{-/Y}$ and littermate control mice, as described (12), with the exception that purified anti-IL-7Rα antibody (A734; eBioscience, San Diego, CA) was included in the lineage depletion. A portion of sorted CMPs were cultured in Methocult GF M3434 (StemCell Technologies) methylcellulose supplemented with 20 ng/ml human Flt3L (Peprotech). The remainder was cultured in StemSpan media supplemented with 100 ng/ml stem cell factor/20 ng/ml Flt3L/20 ng/ml IL-3/20 ng/ml IL-6/100 ng/ml thrombo poietin for 5 days before culturing in supplemented M3434 methylcellulose. Methylcellulose cultures received equal numbers of input CMP before and after expansion. CFU-GM, burst-forming unit erythroid (BFU-E), and CFU-granulocyte/erythroid/macrophage/megakaryocyte (CFU-GEMM) were all present in day 0 cultures. Only CFU-GM were present in day 5 cultures. Therefore, only CFU-GM numbers were used to determine expansion of CMP. The expansion in the number of CMP-derived CFU-GM after 5 days in culture was calculated by dividing the average number of CFU-GM/1,000 CMP at day 5 by

the average number of CFU-GM/1000 CMP at day 0. *P* values were generated by Student's *t* test.

Analysis of Primitive Hematopoietic Populations in Hmgb3$^{-/Y}$ Mice After 5-FU Treatment. Eight- to ten-week-old *Hmgb3*$^{-/Y}$ and littermate wild-type mice were injected i.p. with 150 mg/kg 5-FU (the standard dose for all experiments; Sigma, St. Louis, MO). Two, four, six, and eight days after treatment, mice were killed and their bone marrow analyzed for the presence of HSC, CLP, and CMP populations. Cell staining and detection of the HSC (lin$^-$, c-kit^{HI}, Sca-1^{HI}, and IL-7Rα^-), CLP (lin$^-$, c-kit^{LO}, Sca-1^{LO}, and IL-7Rα^+), and CMP (lin$^-$, c-kit$^+$, Sca-1$^-$, and IL-7Rα^-) populations were performed as described (13). Unless specified, flow cytometry analysis for this and all other experiments was performed on a FACSCalibur (Becton Dickinson) by using 488-nm argon and 633-nm helium-neon lasers. *P* values were generated by Student's *t* test.

Analysis of Primitive Hematopoietic Populations in Hmgb3$^{GFP/Y}$ Mice After 5-FU Treatment. Lin$^-$ cells were isolated from groups of three untreated 8- to 10-week-old *Hmgb3*$^{GFP/Y}$ and littermate wild-type mice 4 days after 5-FU administration and were stained with APC-conjugated c-kit (2B8: PharMingen, San Diego, CA) and phycoerythrin-conjugated Sca-1 (E13–161.7: PharMingen), as described (12), before analysis by flow cytometry. *P* values were generated by Student's *t* test.

Competitive Bone Marrow Transplants. Bone marrow cells were pooled from groups of three untreated wild-type and *Hmgb3*$^{-/Y}$ mice and wild-type and *Hmgb3*$^{-/Y}$ mice 4 days after 5-FU treatment. Lineage depletion and staining for c-kit and Sca-1 were performed as described (12). Cells were sorted into lin$^-$, Sca-1$^+$, and c-kit^{HI} or c-kit^{NEG} populations. Sorted cells (1×10^4) were transplanted along with 1×10^6 B6.SJL-*Ptprc*^{a}/BoAiTac bone marrow cells into lethally irradiated (990 rad, Cs^{137} source) 129SvEvTac $\times$ B6.SJL-*Ptprc*^{a}/BoAiTac F1 recipients. Twelve weeks later, contribution of donor and competitor HSCs toward repopulation was determined by staining recipients' bone marrow with phycoerythrin-conjugated anti-CD45.1 (A20, PharMingen) and PerCP-Cy5.5-conjugated anti-CD45.2 (104, PharMingen) before analysis by flow cytometry. *P* values were generated by Student's *t* test.

Analysis of HSC Cell Cycle Status. Bone marrow cells from groups of five 8- to 10-week-old *Hmgb3*$^{-/Y}$ and littermate wild-type mice were pooled together 2 and 4 days after 5-FU treatment. Lineage depletion was performed as described, with the exception that purified anti-IL-7Rα was included in the depletion, and purified anti-Mac-1 was not (17, 24). Staining for the SP phenotype by using Hoescht dye was performed as described (23). After Hoescht staining, cells were stained with phycoerythrin-conjugated anti-Sca-1. Cells were sorted on a FACS Vantage SE (Becton Dickinson) by using UV (100 mW) and 488-nm argon lasers. Sorted lin$^-$, SP$^+$, Sca-1$^+$, and IL-7Rα^- cells were immediately stained with propidium iodide by using the NuCycl PI staining kit (Exalpha Biologicals, Watertown, MA) according to the manufacturer's instructions before analysis by flow cytometry. Cell cycle data analysis was performed by using ModFit software (Verity Software, Topsham, ME). *P* values were generated by Student's *t* test.

Analysis of HSC Proliferation. Groups of three *Hmgb3*$^{-/Y}$ or littermate wild-type mice were injected with a single dose of 1 mg of BrdU (PharMingen) i.p. 2 and 4 days after treatment with 5-FU. Eighteen hours later, bone marrow was harvested and lin$^-$, SP$^+$, and IL-7Rα^- sorted as described above. Sorted cells were stained with APC-conjugated anti-Sca-1 (D7, eBioscience) before the cells were fixed and stained with a FITC-conjugated anti-BrdU antibody by using the FITC BrdU Flow Kit (PharMingen) according to the manufacturer's instructions before analysis by flow cytometry. *P* values were generated by Student's *t* test.

RT-PCR. Bone marrow cells were harvested from 8- to 10-week old TOPGAL $\times$ *Hmgb3*$^{-/Y}$ or littermate TOPGAL wild-type mice. Lineage depletion (which included purified anti-IL-7Rα), Hoescht dye staining for the SP phenotype, and antibody staining with anti-c-kit and Sca-1 were performed as described above. RNA was isolated from sorted HSCs (Lin$^-$, SP+, c-kit$^+$, Sca-1$^+$, and IL-7Rα^-) by using TRIzol (Invitrogen, Carlsbad, CA) according to the manufacturer's instructions. RT-PCR was performed as described by using a duplex-PCR with one primer pair amplifying the test gene and the second primer pair amplifying β2-microglobulin as an internal control. Limiting dilutions of HSC mRNA were used to ensure amplifications remained within the linear range. Primer pairs used for gene amplification were: 5′-GGCTGTAGAGCGAGTGTTGC-3′ (sense) and 5′-GTAGAGGTTGACAGTGTAGAT-3′ (anti-sense) for *lacZ* (27), 5′-AAGCACAAATGCCGTCGTC-3′ (sense) and 5′-CAGCGTCGTCATTGCTCATG-3′ (anti-sense) for *Dvl1*, and 5′-TGGGCAACATGATGGTTGTG-3′ (sense) and 5′-GCTGTCTTGAGACTCATGGA-3′ (anti-sense) for β2-microglobulin (28). Reactions were performed for 32 cycles at 94° for 30 sec, 64° for 30 sec, and 72° for 30 sec. *LacZ* and *Dvl1* mRNA levels were measured and normalized to β2-microglobulin by performing densitometry on relative band intensities. RT reactions performed without enzyme served as negative controls for genomic DNA amplification.

1. Kondo M, Wagers AJ, Manz MG, Prohaska SS, Scherer DC, Beilhack GF, Shizuru JA, Weissman IL (2003) *Annu Rev Immunol* 21:759–806.
2. Bustin M, Lehn DA, Landsman D (1990) *Biochim Biophys Acta* 1049:231–243.
3. Vaccari T, Beltrame M, Ferrari S, Bianchi M (1998) *Genomics* 49:247–252.
4. Ronfani L, Ferraguti M, Croci L, Ovitt CE, Scholer HR, Consalez GG, Bianchi ME (2001) *Development (Cambridge, UK)* 128:1265–1273.
5. Bianchi ME, Beltrame M, Paonessa G (1989) *Science* 243:1056–1059.
6. Pil PM, Lippard SJ (1992) *Science* 256:234–236.
7. Zappavigna V, Falciola L, Citterich MH, Mavilio F, Bianchi ME (1996) *EMBO J* 15:4981–4991.
8. Zwilling S, Konig H, Wirth T (1995) *EMBO J* 14:1198–1208.
9. Antonchuk J, Sauvageau G, Humphries R (2001) *Exp Hematol* 29:1125–1134.
10. Niwa H, Miyazaki J, Smith AG (2000) *Nat Genet* 24:372–376.
11. Calogero S, Grassi F, Aguzzi A, Voigtlander T, Ferrier P, Ferrari S, Bianchi ME (1999) *Nat Genet* 22:276–280.
12. Nemeth MJ, Curtis DJ, Kirby MR, Garrett-Beal LJ, Seidel NE, Cline AP, Bodine DM (2003) *Blood* 102:1298–1306.
13. Nemeth MJ, Cline AP, Anderson SM, Garrett-Beal LJ, Bodine DM (2005) *Blood* 105:627–634.
14. Logan CY, Nusse R (2004) *Annu Rev Cell Dev Biol* 20:781–810.
15. Reya T, Duncan AW, Ailles L, Domen J, Scherer DC, Willert K, Hintz L, Nusse R, Weissman IL (2003) *Nature* 423:409–414.
16. Jamieson CH, Ailles LE, Dylla SJ, Muijtjens M, Jones C, Zehnder JL, Gotlib J, Li K, Manz MG, Keating A, *et al.* (2004) *N Engl J Med* 351:657–667.
17. Randall TD, Weissman IL (1997) *Blood* 89:3596–3606.
18. Muench M, Moore M (1992) *Exp Hematol* 20:611–618.
19. Iscove NN, Shaw AR, Keller G (1989) *J Immunol* 142:2332–2337.
20. Kondo M, Weissman IL, Akashi K (1997) *Cell* 91:661–672.
21. Akashi K, Traver D, Miyamoto T, Weissman I (2000) *Nature* 404:193–197.
22. DasGupta R, Fuchs E (1999) *Development (Cambridge, UK)* 126:4557–4568.
23. Goodell MA, Brose K, Paradis G, Conner AS, Mulligan RC (1996) *J Exp Med* 183:1797–1806.
24. Uchida N, Dykstra B, Lyons K, Leung F, Kristiansen M, Eaves C (2004) *Blood* 103:4487–4495.
25. Yanagawa S, van Leeuwen F, Wodarz A, Klingensmith J, Nusse R (1995) *Genes Dev* 9:1087–1097.
26. Lee JS, Ishimoto A, Yanagawa S (1999) *J Biol Chem* 274:21464–21470.
27. Aird WC, Edelberg JM, Weiler-Guettler H, Simmons WW, Smith TW, Rosenberg RD (1997) *J Cell Biol* 138:1117–2114.
28. Orlic D, Anderson S, Biesecker LG, Sorrentino BP, Bodine DM (1995) *Proc Natl Acad Sci USA* 92:4601–4605.